Nanomed Res J 8(4):335-344, Autumn 2023

RESEARCH ARTICLE

Encapsulation of Beta-lactam Antibiotic Amoxicillin in Chitosan-alginate Nanohydrogels to Improve Antibacterial Efficacy

Koyeli Girigoswami, Agnishwar Girigoswami*

Medical Bionanotechnology, Faculty of Allied Health Sciences, Chettinad Hospital and Research Institute (CHRI), Chettinad Academy of Research and Education (CARE), Kelambakkam, Chennai, TN-603103, India

ARTICLE INFO

Article History:
Received 01 Jun 2023
Accepted 18 Jul 2023
Published 01 Aug 2023

Keywords:
Chitosan
Alginate
Amoxicillin
Nanohydrogels
Polymeric nanoparticles

ABSTRACT

Nanotechnology offers several opportunities to improve conventional drugs to avoid issues that pharmaceutical industries are facing nowadays. Hydrophobic and hydrophilic drugs have been found to be more readily soluble in mixed polymer nanohydrogels, which improves their solubility in solution. An attempt has been made in the present study to enhance the efficacy of beta-lactam antibiotics by making nanoformulation using mixed polymer nanohydrogels derived from natural polymers sodium alginate and chitosan. As a consequence, this formulation permitted amoxicillin (MOX) to be entrapped in alginate hydrogels and, in addition, chitosan-induced cationic charges on the surface of nanoparticles. Physicochemical characterizations and swelling properties, encapsulation efficiency, MOX release profile at different pH, and MTT assay to establish the toxicity of synthesized nanocomposite were investigated. There was a significant improvement in the effectiveness of the encapsulated drug amoxicillin against Gram-negative bacteria *Escherichia coli* compared to the aqueous solution of the drug. It has been calculated that the encapsulation efficiency was approximately 64% by spectrophotometry, and antibiotic sensitivity tests in the presence of Gram-negative bacteria have shown that the encapsulated drug within nanohydrogels has superior antibacterial efficacy against them. This formulation with cationic surface charge may be a superior alternative to inactivate beta-lactam antibiotic-resistant Gram-negative bacteria than the standard medications available.

How to cite this article
Girigoswami K., Girigoswami A. Encapsulation of Beta-lactam Antibiotic Amoxicillin in Chitosan-alginate Nanohydrogels to Improve Antibacterial Efficacy. Nanomed Res J, 2023; 8(4): 335-344. DOI: 10.22034/nmrj.2023.04.002

INTRODUCTION

A number of applications of nanotechnology have emerged in medicine over the last few decades, including applications for diagnosis, treating, and targeting diseased cells like tumors in a safe and efficient manner. As a result of nanoparticles being used in the delivery of drugs, they have demonstrated a number of advantages over traditional drug delivery systems that include good pharmacokinetics, enhanced solubility, reduced side effects, and a new dimension to drug resistance [1, 2]. There are several types of nanoparticles that are used in drug delivery, and their physicochemical characteristics, selection of materials, and fabrications are usually dictated by the pathophysiology of diseased conditions. It is understood that nanodelivery vehicles or nanocarriers, which are used in cancer treatment, target cancerous cells by using the carrier effect of nanoparticles and the positioning properties of targeting molecules after they are absorbed, resulting in the destruction of cancerous cells. The nanoparticles also offer a platform for encapsulating drugs or other payloads that are poorly soluble in order to facilitate their delivery to the bloodstream [3-5]. Nanocarriers have been shown to increase the half-life of drugs and induce their accumulation into targeted tissues because of their size, surface characteristics, and ability to enhance permeability and retention. Due to the targeting properties of nano-enabled drug delivery systems, normal cells

* Corresponding Author Email: *agnishwarg@gmail.com*

are protected from the toxicity caused by drugs, which is a major factor in reducing the side effects associated with the treatment of cancer [6, 7]. Nanoformulation of neutraceuticals also shows a beneficial effect on human health compared to bare neutraceuticals [8].

In order to develop new drug molecules, it is necessary to invest a lot of money and time with the least hope [9]. At the same time, regulatory authorities are another barrier in the process of the development of new drugs. Therefore, researchers have used various methods to improve the efficacy-to-safety ratio of drugs in use, including titration of dosages, individualization of drug therapy, and therapeutic drug monitoring. Other very attractive methods have been pursued vigorously, such as sustained or controlled delivery of drugs with zero order kinetics and targeted delivery using several biocompatible delivery vehicles [10, 11]. In this context, submicron-sized colloidal drug carriers are flourishing with increased attention owing to their capability to alter the basic properties and bioactivity of life-saving drugs [12]. They offer improved solubility, stability, pharmacokinetics, and bio-distribution with reduced toxicity profiles [13-15]. The other achievements of nanosized drug carriers are site-specific delivery of therapeutic agents with a sustained or controlled manner [16-18]. In this direction, metal and metal-oxide nanoparticles, liposomes, dendrimers, polymeric nanoparticles, and solid-lipid nanoparticles are promising carriers [13, 19-21].

Polymeric nanoparticles are very promising in drug delivery. It is used to encapsulate drug candidates and deliver them to the targeted tissues with controlled or sustained release of therapeutics [22, 23]. The encapsulation of drugs has been done either after the formation of nanoparticles or during the formation of polymer nanoparticles. The choice of method depends on the physicochemical properties of drugs as well as polymer components [24]. There are several natural polymers that are used for the entrapment of drugs, considering their biocompatibility and bioavailability. Chitosan, alginate, cellulose, collagen, poly (d, l-lactide-co-glycolic acid), poly(ethyl cyanoacrylate), poly(butyl cyanoacrylate), poly(isobutyl cyanoacrylate), polyvinyl alcohol, polycaprolactone, polyglycolic acids, etc. are very commonly used polymers in designing drug delivery systems. It is possible to control the properties of polymer nanoparticles by changing their composition, limit of polymerization, and sensitivity towards external stimuli [25-27].

Beta-lactams are a group of antibiotics containing beta-lactam rings in their active structures. This reactive group contains 3-carbons, one nitrogen in their ring [28, 29]. Beta-lactam antibiotics are one of the most commonly prescribed drugs in the world. This group of antibiotics inhibits the synthesis of peptidoglycans. It inhibits the last step of peptidoglycan synthesis by acylating the transpeptidase involved in cross-linking peptides for the formation of peptidoglycans [30]. The peptidoglycan is an active component for the formation of bacterial cell walls, mainly in Gram-positive bacteria. Therefore, cell wall synthesis stops in the absence of peptidoglycan, and the bacteria die. The targets for the action of beta-lactam antibiotics are called PBP (penicillin-binding proteins). Common examples of beta-lactam antibiotics are Penicillins, Cephalosporins, Carbapenems, and Monobactams [29]. Several studies have documented that the pattern of antibiotic usage, including overuse of broad-spectrum antibiotics like beta-lactams, induces the development of antibiotic resistance [31].

Antibiotic resistance is a major cause of health hazards worldwide, especially in developing countries [32, 33]. There are practical pieces of evidence on the direct relationship between antibiotic consumption on an irregular basis with improper dosages and the growing antibiotic resistance to several strains of bacteria. Incorrectly prescribed drugs are also contributing to the generation of resistant bacteria strains. Study shows that drug choice and therapy duration are the two major parameters in antibiotic therapy [34, 35]. That is why incorrectly prescribed antibiotics have questionable therapeutic benefits. Proper dosage or concentration is another promoter of resistance that induces genetic alterations, and antibiotics lose their sensitivity against the bacteria. Therefore, the pharmaceutical industry faces lots of challenges in resolving these issues with conventional antibiotics. Considering the importance of the same and the advancement of nanoenabled drug delivery systems, the current research has been designed to encapsulate beta-lactam antibiotic amoxicillin by mixed polymeric chitosan-alginate (CA) nanoparticles.

MATERIALS AND METHODS

Alginate, chitosan, amoxicillin, calcium chloride,

yeast extract, bacto tryptone, lysogeny broth, bacto agar, Mueller Hinton agar, 3-(4,5-dimethylthiazol-2-yl)-2,5-diphenyltetrazolium (MTT), antibiotic and antimycotic solution, Dulbecco's Modified Eagle Medium (DMEM/ AL006A), staining dyes were purchased from Himedia, India, and were used as received. The fetal bovine serum (FBS) was procured from Gibco, USA. The *Escherichia coli* (*E. coli*) bacterial strain was collected from the Department of Microbiology, CHRI. Shimadzu UV-1800 UV-vis spectrophotometer was used for the optical studies, and the hydrodynamic size of the synthesized particles in colloidal solution was measured using a Malvern ZS-90 particle size analyzer equipped with a 633 nm laser source following the principle of dynamic light scattering. The photon correlation spectroscopic principle was used to calculate the polydispersity index. TESCAN Vega scanning electron microscope was used for capturing images of nanoparticles. A Robonik Readwell Touch automatic ELISA plate analyzer was used for the MTT assay.

Synthesis of Chitosan-Alginate Mixed Polymer Nanoparticles

CA nanoparticles were prepared using the standard protocol with required modifications [24]. The natural polymer chitosan was dissolved in a 1% acetic acid solution, followed by a pH adjustment of 5.4 using a dilute solution of sodium hydroxide. The sodium alginate solution was prepared in autoclaved deionized water, and the pH was adjusted to 5.1 using a dilute solution of hydrochloric acid. The mixed polymeric nanoparticles CA were prepared by a two-step method. 4 ml aqueous calcium chloride (3.35 mg/ml) solution was added dropwise to the 20 ml alginate solution (0.8 mg/ml) in the presence of amoxicillin with continuous stirring. After 30 min, 8 ml of chitosan solution (0.8 mg/ml) was added to the above alginate mixture with stirring for an additional hour. The transition to opalescent suspension is the indication of the formation of mixed polymeric CA nanoparticles. The suspension was equilibrated overnight for the uniform size distribution, which was confirmed by the particle size analyzer. The synthesized nanoformulations were centrifuged at 12000 rpm for 20 min. The pellet was collected and dispersed in 10 ml of sterile deionized water, and the process was repeated three times to remove the unreacted polymers and unbound drugs. The amoxicillin (MOX) was added to the synthesized particles and sonicated for 30 min to load the drug in the mixed polymer nanoparticles (CA-MOX).

Swelling Assay, Encapsulation Efficiency, and In-vitro Drug Release Kinetics

The encapsulation efficiency was measured spectrophotometrically. The wavelength was fixed at the λ_{max} of amoxicillin, which was 272 nm. The capacity of water sorption of CA-MOX was carried out by swelling the cryodessicated CA-MOX in PBS (pH=7.4) and in an HCl/KCl buffer of pH 2.2 at room temperature for 300 min. The in vitro drug release kinetics were studied using standard protocol [21, 36]. The amoxicillin-loaded CA nanoparticles were sealed in a porous dialysis membrane, and the release of amoxicillin was allowed in 25 ml PBS of pH 7.4 and 2.2 at room temperature. 2 ml of drug-containing PBS was collected at a predetermined time interval to measure the optical density at 272 nm. The cumulative release of amoxicillin was plotted against the time interval [37, 38].

Cell viability assay

The HepG2 cells were plated in a 96-well plate adding $4'10^5$ cells/ml in DMEM medium supplemented with 10% of FBS and 1% antibiotic and antimycotic solutions at 37°C and 5% CO_2 in a humidified atmosphere [1]. The cells were then treated with CA and CA-MOX of variable concentrations from 3 µg/ml to 60 µg/ml. After 24h of incubation, 5 mg/ml of MTT was added and further incubated for four hours. Finally, 100 µl of DMSO was added to each well in order to solubilize blue-colored formazan precipitate to study the absorbance at 570 nm using a microplate reader.

Antibiotic Sensitivity Test

The antibiotic sensitivity test was carried out with encapsulated amoxicillin and the free one. The antibiotic susceptibility patterns against *E. coli* were established in vitro using the well-diffusion method on Mueller-Hinton agar plate. After the inoculation, the plate surface was dried by placing the plate in the incubator for 15 min. Wells were made then on the inoculated plate, and the wells were filled with 100 µl encapsulated amoxicillin and free amoxicillin separately with increasing concentration, taking the first well as control. The plates were kept overnight in the incubator at 37°C. The zone of inhibition was measured after overnight incubation [39, 40].

RESULTS AND DISCUSSION

Alginate is a biodegradable soluble linear polysaccharide that is made of the 1-4 linked α-L-guluronic and β-D-mannuronic acid. Alginate forms a physically cross-linked gel in the presence of calcium ions that bind mostly G-block residues. Alginate generally forms microscopic beads in the presence of calcium ions. Smaller-sized particles or particles with narrow size distribution can be prepared by complexing chitosan-like highly charged poly-cations. Therefore, in the present study, mixed polymer CA nanoparticles have been prepared to encapsulate beta-lactam antibiotics.

Structural and Morphological Characterization

The ATR-FTIR spectroscopy was adopted to characterize the potential interaction present in the synthesized mixed nanocarriers CA (Fig. 1). The characteristic peaks at 3419 cm^{-1} correspond to the $-NH_2$ and –OH stretching. The peak at 2877 cm^{-1} was due to the –CH stretching, and the band at 1632 cm^{-1} and 1574 cm^{-1} represent the carbonyl stretching and N-H bending vibrations, respectively. The N-H stretching of amide and ether bonds was observed at 1414 cm^{-1} and 1354 cm^{-1}. The characteristic peaks observed at 1078 cm^{-1} and 1029 cm^{-1} were for the secondary and primary hydroxyl groups present as the cyclic alcohols in the mixed CA hydrogel. The presence of all the characteristic IR bands confirms the formation of CA nanocarriers.

The hydrodynamic diameter of the synthesized CA (Fig 2) was measured using a particle size analyzer, and the size was 220 nm, whereas the

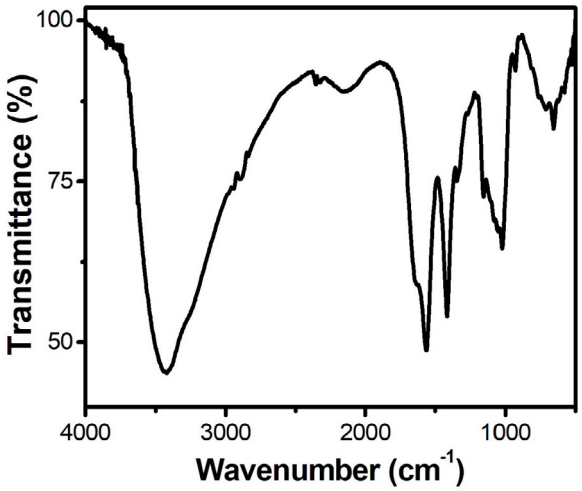

Fig. 1. Fourier Transformed Infrared spectra of CA nanoparticles.

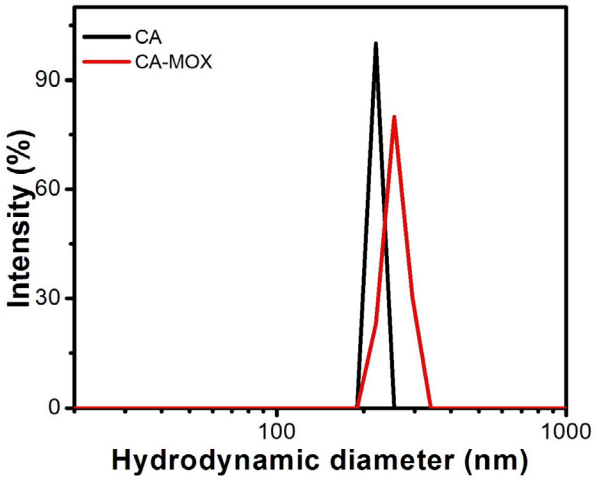

Fig. 2. Particle size distribution measured by dynamic light scattering method for CA and CA-MOX

Fig. 3. Scanning electron micrograph of CA-MOX nanoparticles to support the morphology.

hydrodynamic diameter became 255 nm after the encapsulation of amoxicillin (CA-MOX). The polydispersity index (PDI) was calculated from the photon-correlated spectroscopic analysis, which was 0.17 and 0.22, respectively, for CA and CA-MOX [41]. The PDI values indicated the monodispersed CA particle distribution. The zeta-potential values of -42 mV and -23 mV for CA and CA-MOX, respectively, indicate the stability of the formulations.

The surface morphology was characterized using scanning electron microscopy. SEM image (Fig. 3) showed the formation of CA nanoparticles. The CA particles were seen to be spherical, distinct, and regularly distributed. The mean diameter was calculated as 150 ± 15.27 nm. The hydrodynamic diameter obtained from the DLS measurement represents the size of the particles in the colloidal solution. On the other hand, an SEM image shows the actual diameter, which differs from the obtained hydrodynamic diameter predictably.

Spectrophotometric and spectrofluorimetric studies

Spectrophotometric studies were done using a UV-vis spectrophotometer to identify the characteristic peaks for MOX. The maximum absorption bands (λ_{max}) were observed at 272 nm and 227 nm (Fig. 4A). The lower energy band at 272 nm was a structured band, and we continued our further studies with this absorption wavelength. The absorption spectra of CA-MOX showed a higher absorption band at both wavelengths for the same concentration of MOX. Definitely, the molar extinction coefficient was responsible for the same, which depends on the microenvironment around the drug molecules. It is then can be proposed that the drug molecules were encapsulated in the CA polymeric matrix, and the increment in the absorption is proof of it. Since steady-state fluorescence is more sensitive than spectrophotometric measurements, steady-state fluorescence measurements were performed to support further and confirm antibiotic encapsulation predictions (Fig. 4B). MOX showed a peak at 300 nm upon exciting at the λ_{max} = 272 nm. There was a six-fold increment in the emission intensity of CA-MOX, which confirmed the encapsulation. The excitation spectra peaking at 272 nm resembled the absorption spectra for both MOX and CA-MOX fixing λ_{em} = 300 nm.

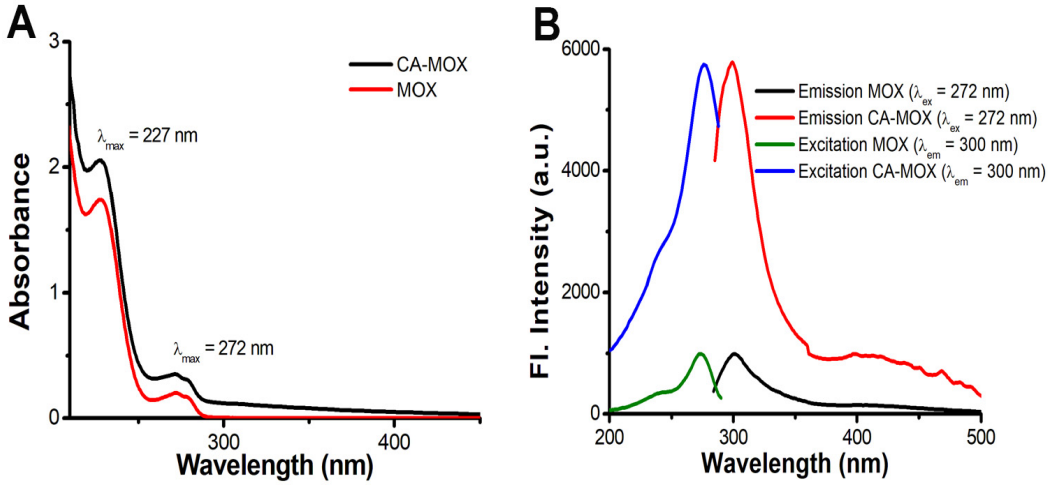

Fig. 4. (A) MOX and CA-MOX absorption spectra to find out the maximum absorption peak. (B) Emission spectra were recorded from steady-state fluorescence measurement to find out the maximum emission intensity and to confirm the encapsulation

Swelling tests

The swelling assays of CA-MOX were conducted in PBS (pH=7.4) at room temperature. The equilibrium mass swelling of CA-MOX was calculated after overnight incubation by the equation given below:

Percent equilibrium mass swelling =
$[\{(m_1-m_0)/m_0\} \times 100]$

Where m_0 and m_1 are the mass weight of vacuum-dried gel at 45°C and swollen gel, respectively [42]. The mass swelling at pH 7.4 was initially higher with time, and later, it became almost similar (Fig. 5). Hydration of hydrophilic groups in alginate and chitosan is the principal cause of the swelling behavior of AC-MOX complexes. There has been free water penetration into the CA-MOX, and it has filled the empty spaces in the polymeric matrix, in turn causing the CA-MOX to swell. When there is a high degree of interaction between two polymeric chains in the mixed polymeric nanoparticles, the swelling of particles reduces as a result. The higher swelling was observed at pH 2.2 (HCl/KCl buffer) due to the higher rate of protonation of $-NH_2$ groups present in the chitosan and converted to ammonium ions. The osmotic pressure reduced at lower pH due to the like-charge repulsion arising from ammonium ions enhances the swelling behavior of CA-MOX.

Drug Encapsulation and Release Kinetics

The encapsulation efficiency (EE) was calculated spectrophotometrically. The encapsulation efficiency was determined by using the equation given below. The optical density of the drug amoxicillin was monitored at 272 nm, and the EE was found to be 64%. The release kinetics was studied using the method explained in the method section. Figure 6 shows the cumulative drug release in percent against the time intervals in hours for thirty hours. The release profile is very steep in the first couple of hours due to the burst release of loosely bound drugs on the surface of the CA-AMOX nanoformulations. The latter part was very stable and followed the near zero-order kinetics due to the sustained release of amoxicillin. Almost 72% of drugs were released at the end of 18h. In the later period, the release started to decline. In the presence of acidic pH, the release profile initially appeared steeper than at physiological pH and later became steady after 8.5h, indicating sustained release of MOX (Fig. 6). The higher equilibrium mass swelling and the overall cationic charge on the chitosan molecules due to huge protonation might be the cause of better release of amoxicillin at HCl/KCl buffer.

The percent encapsulation efficiency (EE) =
[(Total Drug – Free Drug) / Total Drug] × 100.

Cell viability assay

In order to assess whether CA and CA-MOX are suitable as drug delivery systems, the MTT assay was used to assess the cytotoxicity of CA and CA-MOX using HepG2 cells (Fig. 7). Both CA

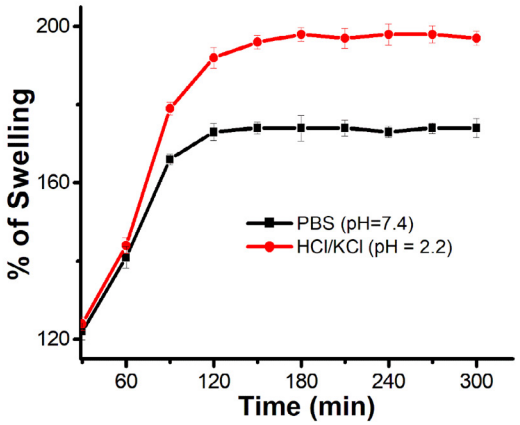

Fig. 5. Percentage swelling of CA-MOX in PBS (pH=7.4) and HCl/KCl buffer (pH=2.2),

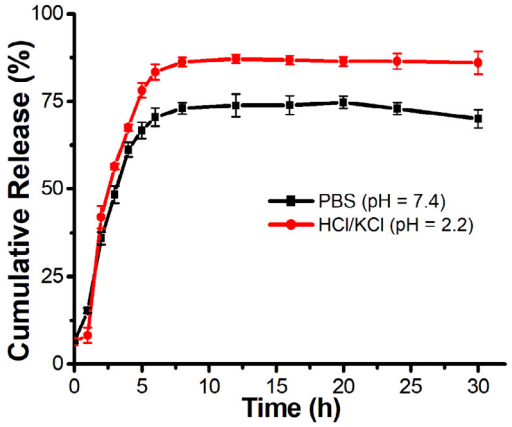

Fig. 6. Cumulative amoxicillin release profile from the CA nanoparticles in two different pH.

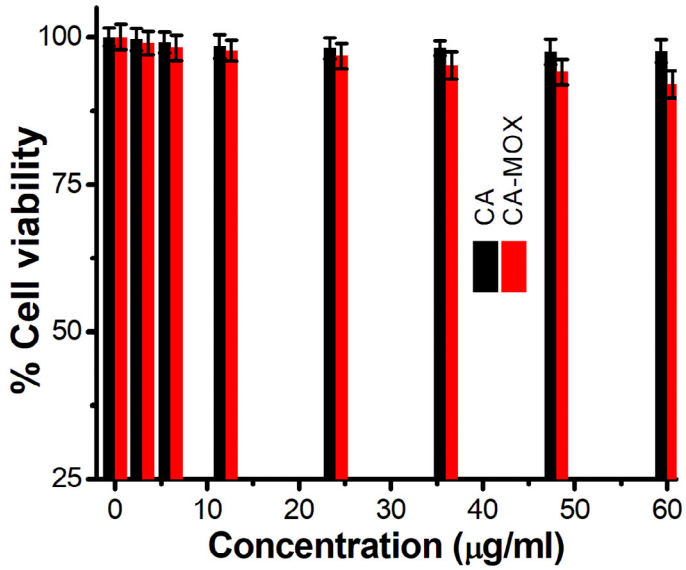

Fig. 7. A. Cell viability study using MTT assay on HepG2 cell line

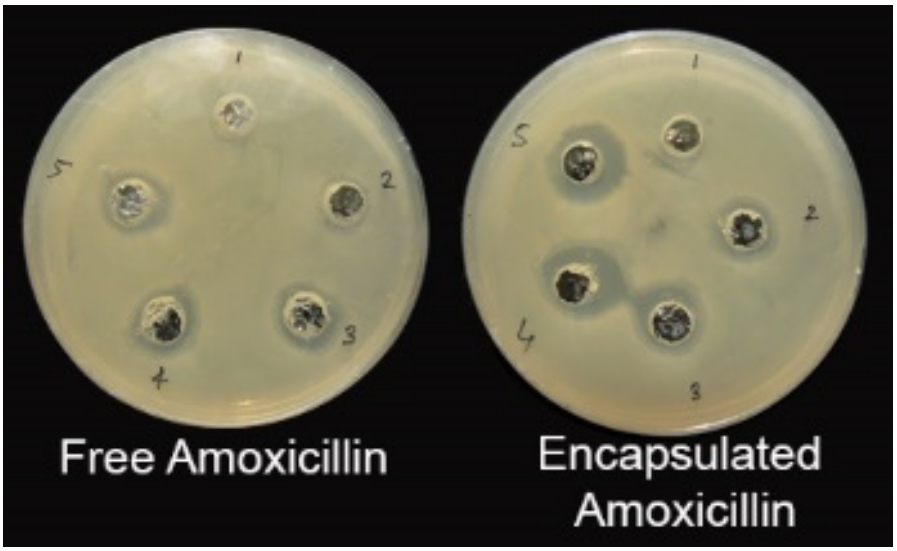

Fig. 8. Antibiotic sensitivity assay using well-diffusion method

Table 1. Zones of inhibition calculated to establish the effective role of CA-MOX

Well No.	Drug Con. mg/ml	Free amoxicillin			Amoxicillin encapsulated in CA nanoparticles		
		D1 cm	D2 cm	Avg. cm	D1 cm	D2 cm	Avg. cm
1	0.00	0.91	0.92	0.915 ± 0.007	0.90	0.91	0.905 ± 0.007
2	0.10	0.91	0.90	0.905 ± 0.007	1.10	1.20	1.15 ± 0.071
3	0.20	0.90	0.91	0.905 ± 0.007	1.40	1.20	1.30 ± 0.141
4	0.40	1.00	1.10	1.05 ± 0.070	1.50	1.40	1.45 ± 0.071
5	0.80	1.40	1.50	1.45 ± 0.071	2.00	1.60	1.80 ± 0.283

and the formulation CA-MOX showed negligible toxicity after 24 hours of incubation at different concentrations ranging from 3 µg/ml to 60 µg/ml, under physiological conditions maintained at CO_2 incubator. Comparatively, CA-MOX was more effective at killing HepG2 cells than CA in the same study, but the inhibitory effect of CA-MOX is negligibly smaller and not significant in terms of toxicity. Therefore, the formulations can be used as drug-delivery vehicles to deliver beta-lactam antibiotics.

Antibiotics Sensitivity Assay

The well-diffusion method was applied to check the antibacterial activity of amoxicillin and amoxicillin encapsulated in alginate-chitosan nanoparticles. Five wells were made, and the drug was added with increasing concentrations as 0 mg/ml, 0.1 mg/ml, 0.2 mg/ml, 0.4 mg/ml, and 0.8 mg/ml (Fig. 8). The zones of inhibition were measured after overnight incubation in two possible directions and finally, the average was taken for the discussion of results to establish the potential antibacterial activities of encapsulated drugs. The results are given in Table 1.

At the concentration zero, there was no zone of inhibition. The well size was measured as 0.9 cm. The zone of inhibition started to be observed at well no. 3 in the case of bare amoxicillin. Further increase in concentration generated a bigger zone, and finally, it was 1.45 cm at well no. 5, where the concentration of amoxicillin was 0.8 mg/ml. In the case of encapsulated drugs, the zone of inhibitions started at the 2nd well itself, and gradually, it increased with the increasing concentration of amoxicillin. At the final well, where the concentration of the encapsulated drug was 0.8 mg/ml, the zone became 1.8 cm in diameter. It was clear that the antibacterial activity of the encapsulated drug was more than that of the normal drug.

CONCLUSIONS

The current experiment successfully demonstrated the improved efficacy of encapsulated amoxicillin in the alginate-chitosan nanoparticles, which can efficiently resolve the limitations of beta-lactam antibiotics. Spectrophotometric and fluorimetric observations established the encapsulation of drugs in the CA scaffolds. The hydrodynamic diameter of the synthesized particles was 220 nm before encapsulation, and it became 255 nm after the encapsulation of the beta-lactam drug MOX. The encapsulation efficiency was 64%, which was measured spectrophotometrically, and there was an initial burst release followed by a nearly zero-order release of the drug for a period of 30 h. The formulation showed better swelling behavior and the MOX release profile in HCl/KCl buffer (pH = 2.2) compared to PBS of pH 7.4, and the safety of using CA-MOX as a drug delivery system was established by the cell viability assay using HepG2 cell lines. The well-diffusion method was employed to check the antibacterial activity, and it was observed that the encapsulated formulations have superior antibacterial activity against *E. coli*. Therefore, the combination of enhanced solubility of amoxicillin, biocompatibility, antibacterial efficacy, and a pH-sensitive sustained release profile makes CA-MOX an excellent alternative for treating multidrug resistance and clarifies its superiority over other formulations.

CONFLICT OF INTEREST

The authors declare no conflict of interest.

ACKNOWLEDGMENT

The authors acknowledge CARE for financial and infrastructural support.

REFERENCES

1. Gowtham P, Girigoswami K, Pallavi P, Harini K, Gurubharath I, Girigoswami A. Alginate-Derivative Encapsulated Carbon Coated Manganese-Ferrite Nanodots for Multimodal Medical Imaging. Pharmaceutics. 2022;14(12):2550. https://doi.org/10.3390/pharmaceutics14122550
2. Harini K, Girigoswami K, Girigoswami A. Nanopsychiatry: Engineering of nanoassisted drug delivery systems to formulate antidepressants. International Journal of Nano Dimension. 2022.
3. Singh R, Prasad A, Kumar B, Kumari S, Sahu RK, Hedau ST. Potential of Dual Drug Delivery Systems: MOF as Hybrid Nanocarrier for Dual Drug Delivery in Cancer Treatment. ChemistrySelect. 2022;7(36):e202201288. https://doi.org/10.1002/slct.202201288
4. Vedakumari SW, Senthil R, Sekar S, Babu CS, Sastry TP. Enhancing anti-cancer activity of erlotinib by antibody conjugated nanofibrin-in vitro studies on lung adenocarcinoma cell lines. Mater. Chem. Phys. 2019;224:328-33. https://doi.org/10.1016/j.matchemphys.2018.11.061
5. Banerjee A, Pathak S, Subramanium VD, Dharanivasan G, Murugesan R, Verma RS. Strategies for targeted drug delivery in treatment of colon cancer: current trends and future perspectives. Drug Discov. Today. 2017;22(8):1224-32. https://doi.org/10.1016/j.drudis.2017.05.006
6. Alrushaid N, Khan FA, Al-Suhaimi EA, Elaissari A. Nanotechnology in cancer diagnosis and treatment. Pharmaceutics. 2023;15(3):1025. https://doi.org/10.3390/pharmaceutics15031025
7. Alshammari MK, Almomen EY, Alshahrani KF, Altwalah SF, Kamal M, Al-Twallah MF, et al. Nano-Enabled Strategies for the Treatment of Lung Cancer: Potential Bottlenecks and Future Perspectives. Biomedicines. 2023;11(2):473. https://doi.org/10.3390/biomedicines11020473
8. Balasubramanian D, Girigoswami A, Girigoswami K. Nano resveratrol and its anticancer activity. Current Applied Science and Technology. 2023:10-55003. https://doi.org/10.55003/cast.2022.03.23.010
9. Park H, Otte A, Park K. Evolution of drug delivery systems: From 1950 to 2020 and beyond. J. Controlled Release. 2022;342:53-65. https://doi.org/10.1016/j.jconrel.2021.12.030
10. Oladipo AO, Lebelo SL, Msagati TA. Nanocarrier design-function relationship: The prodigious role of properties in regulating biocompatibility for drug delivery applications. Chem.-Biol. Interact. 2023:110466. https://doi.org/10.1016/j.cbi.2023.110466
11. Hawthorne D, Pannala A, Sandeman S, Lloyd A. Sustained and targeted delivery of hydrophilic drug compounds: A review of existing and novel technologies from bench to bedside. J. Drug Deliv. Sci. Technol. 2022:103936. https://doi.org/10.1016/j.jddst.2022.103936
12. Din FU, Aman W, Ullah I, Qureshi OS, Mustapha O, Shafique S, Zeb A. Effective use of nanocarriers as drug delivery systems for the treatment of selected tumors. International journal of nanomedicine. 2017:7291-309. https://doi.org/10.2147/IJN.S146315
13. Haribabu V, Farook AS, Goswami N, Murugesan R, Girigoswami A. Optimized Mn-doped iron oxide nanoparticles entrapped in dendrimer for dual contrasting role in MRI. Journal of Biomedical Materials Research Part B: Applied Biomaterials. 2016;104(4):817-24. https://doi.org/10.1002/jbm.b.33550
14. Vimaladevi M, Divya KC, Girigoswami A. Liposomal nanoformulations of rhodamine for targeted photodynamic inactivation of multidrug resistant gram negative bacteria in sewage treatment plant. Journal of Photochemistry and Photobiology B: Biology. 2016;162:146-52. https://doi.org/10.1016/j.jphotobiol.2016.06.034
15. Ghosh S, Girigoswami K, Girigoswami A. Membrane-encapsulated camouflaged nanomedicines in drug delivery. Nanomedicine. 2019;14(15):2067-82. https://doi.org/10.2217/nnm-2019-0155
16. Imperiale JC, Schlachet I, Lewicki M, Sosnik A, Biglione MM. Oral pharmacokinetics of a chitosan-based nano-drug delivery system of interferon alpha. Polymers. 2019;11(11):1862. https://doi.org/10.3390/polym11111862
17. Mishra V, Bansal KK, Verma A, Yadav N, Thakur S, Sudhakar K, Rosenholm JM. Solid lipid nanoparticles: Emerging colloidal nano drug delivery systems. Pharmaceutics. 2018;10(4):191.

https://doi.org/10.3390/pharmaceutics10040191
18. Girigoswami A, Yassine W, Sharmiladevi P, Haribabu V, Girigoswami K. Camouflaged Nanosilver with Excitation Wavelength Dependent High Quantum Yield for Targeted Theranostic. Scientific reports. 2018;8(1):16459. https://doi.org/10.1038/s41598-018-34843-4
19. Sharmiladevi P, Akhtar N, Haribabu V, Girigoswami K, Chattopadhyay S, Girigoswami A. Excitation wavelength independent carbon-decorated ferrite nanodots for multimodal diagnosis and stimuli responsive therapy. ACS Applied Bio Materials. 2019;2(4):1634-42. https://doi.org/10.1021/acsabm.9b00039
20. Haribabu V, Sharmiladevi P, Akhtar N, Farook AS, Girigoswami K, Girigoswami A. Label free ultrasmall fluoromagnetic ferrite-clusters for targeted cancer imaging and drug delivery. Current drug delivery. 2019;16(3):233-41. https://doi.org/10.2174/1567201816666181119112410
21. Amsaveni G, Farook AS, Haribabu V, Murugesan R, Girigoswami A. Engineered multifunctional nanoparticles for DLA cancer cells targeting, sorting, MR imaging and drug delivery. Advanced Science, Engineering and Medicine. 2013;5(12):1340-8. https://doi.org/10.1166/asem.2013.1425
22. Masood F. Polymeric nanoparticles for targeted drug delivery system for cancer therapy. Materials Science and Engineering: C. 2016;60:569-78. https://doi.org/10.1016/j.msec.2015.11.067
23. Han Z, Lv W, Li Y, Chang J, Zhang W, Liu C, Sun J. Improving tumor targeting of exosomal membrane-coated polymeric nanoparticles by conjugation with aptamers. ACS Applied Bio Materials. 2020;3(5):2666-73. https://doi.org/10.1021/acsabm.0c00181
24. Deepika R, Girigoswami K, Murugesan R, Girigoswami A. Influence of divalent cation on morphology and drug delivery efficiency of mixed polymer nanoparticles. Current drug delivery. 2018;15(5):652-7. https://doi.org/10.2174/1567201814666170825160617
25. Wang Q, Jamal S, Detamore MS, Berkland C. PLGA-chitosan/PLGA-alginate nanoparticle blends as biodegradable colloidal gels for seeding human umbilical cord mesenchymal stem cells. Journal of biomedical materials research Part A. 2011;96(3):520-7. https://doi.org/10.1002/jbm.a.33000
26. Chai F, Sun L, He X, Li J, Liu Y, Xiong F, Ge L, Webster TJ, Zheng C. Doxorubicin-loaded poly (lactic-co-glycolic acid) nanoparticles coated with chitosan/alginate by layer by layer technology for antitumor applications. International Journal of Nanomedicine. 2017:1791-802. https://doi.org/10.2147/IJN.S130404
27. Dang JM, Leong KW. Natural polymers for gene delivery and tissue engineering. Advanced drug delivery reviews. 2006;58(4):487-99. https://doi.org/10.1016/j.addr.2006.03.001
28. Kong KF, Schneper L, Mathee K. Beta-lactam antibiotics: from antibiosis to resistance and bacteriology. Apmis. 2010;118(1):1-36. https://doi.org/10.1111/j.1600-0463.2009.02563.x
29. Pandey N, Cascella M. Beta Lactam Antibiotics. In: StatPearls. StatPearls Publishing, Treasure Island (FL); 2022.
30. Allen N, Hobbs J, Alborn W. Inhibition of peptidoglycan biosynthesis in gram-positive bacteria by LY146032. Antimicrob. Agents Chemother. 1987;31(7):1093-9. https://doi.org/10.1128/AAC.31.7.1093
31. Wilke MS, Lovering AL, Strynadka NC. β-Lactam antibiotic resistance: a current structural perspective. Current opinion in microbiology. 2005;8(5):525-33. https://doi.org/10.1016/j.mib.2005.08.016
32. Ventola CL. The antibiotic resistance crisis: part 1: causes and threats. Pharmacy and therapeutics. 2015;40(4):277.
33. Klein EY, Van Boeckel TP, Martinez EM, Pant S, Gandra S, Levin SA, et al. Global increase and geographic convergence in antibiotic consumption between 2000 and 2015. Proceedings of the National Academy of Sciences. 2018;115(15):E3463-E70. https://doi.org/10.1073/pnas.1717295115
34. Holten KB, Onusko EM. Appropriate prescribing of oral beta-lactam antibiotics. American family physician. 2000;62(3):611-20.
35. Sabath L. Mechanisms of resistance to beta-lactam antibiotics in strains of Staphylococcus aureus. Annals of internal medicine. 1982;97(3):339-44. https://doi.org/10.7326/0003-4819-97-3-339
36. Imperiale JC, Schlachet I, Lewicki M, Sosnik A, Biglione MM. Oral Pharmacokinetics of a Chitosan-Based Nano-Drug Delivery System of Interferon Alpha. Polymers. 2019;11(11):1862. https://doi.org/10.3390/polym11111862
37. Güncüm E, Işıklan N, Anlaş C, Ünal N, Bulut E, Bakırel T. Development and characterization of polymeric-based nanoparticles for sustained release of amoxicillin-an antimicrobial drug. Artificial cells, nanomedicine, and biotechnology. 2018;46(sup2):964-73. https://doi.org/10.1080/21691401.2018.1476371
38. Arora S, Budhiraja R. Chitosan-alginate microcapsules of amoxicillin for gastric stability and mucoadhesion. J. Adv. Pharm. Technol. Res. 2012;3(1):68.
39. Nguyen VT, Vu VT, Nguyen TA, Tran VK, Nguyen-Tri P. Antibacterial activity of TiO2-and ZnO-decorated with silver nanoparticles. Journal of Composites Science. 2019;3(2):61. https://doi.org/10.3390/jcs3020061
40. Bonev B, Hooper J, Parisot J. Principles of assessing bacterial susceptibility to antibiotics using the agar diffusion method. J. Antimicrob. Chemother. 2008;61(6):1295-301. https://doi.org/10.1093/jac/dkn090
41. Jaiganesh T, Rani JDV, Girigoswami A. Spectroscopically characterized cadmium sulfide quantum dots lengthening the lag phase of Escherichia coli growth. Spectrochimica Acta Part A: Molecular and Biomolecular Spectroscopy. 2012;92:29-32. https://doi.org/10.1016/j.saa.2012.02.044
42. Pasparakis G, Bouropoulos N. Swelling studies and in vitro release of verapamil from calcium alginate and calcium alginate-chitosan beads. Int. J. Pharm. 2006;323(1-2):34-42. https://doi.org/10.1016/j.ijpharm.2006.05.054